

## ARTICLES

SnO<sub>2</sub> Nanoparticle-Functionalized Boron Nitride Nanotubes

Chunyi Zhi,\* Yoshio Bando, Chengchun Tang, and Dmitri Golberg

*Advanced Materials Laboratory, National Institute for Materials Science (NIMS), Namiki 1-1, Tsukuba, Ibaraki 305-0044, Japan**Received: November 19, 2005; In Final Form: February 16, 2006*

Boron nitride nanotubes (BNNTs) were synthesized by a carbon-free chemical vapor deposition method using boron and metal oxide as reactants. Then SnO<sub>2</sub> nanoparticles were functionalized on them via a simple wet chemistry method. Detailed transmission electron microscopy (TEM) observations reveal that SnO<sub>2</sub> nanoparticles may cover the tube surface or be encapsulated in tube channels. The lattice distances of both BNNT and SnO<sub>2</sub> have been changed due to the strong interactions between them. The band gap energy of SnO<sub>2</sub> particles is found enlarged due to the size effect and interaction with BNNTs.

## Introduction

Surface functionalization can lead to a significant enhancement of properties relevant to the technological applications of low dimensionality and high surface area materials, such as nanotubes. Intense research has been carried out in an attempt to attach nanoparticles to carbon nanotubes (CNTs). Various approaches have been developed to fabricate SnO<sub>2</sub>, gold, and CdSe, and so forth,<sup>1–4</sup> functionalized CNTs. These functionalized CNTs were suggested to possess potential applications in novel electronic devices, such as transistors, batteries, and molecular computers.

Compared with CNTs, boron nitride nanotubes (BNNTs) have a constant wide band gap,<sup>5</sup> which has been verified by theoretical and experimental work. In addition, BNNTs have high oxidation resistance and structural stability.<sup>6</sup> They are inert to most chemicals. All these features make BNNTs highly useful as a protective sheath for any materials encapsulated within. The extremely high thermal conductivity and superb mechanical properties of BNNT suggest that they may have also applications in nanocomposites.<sup>7–8</sup> Although BNNTs are thought to be highly useful in nanodevices working at elevated temperature and in hazardous environment, the reports on nanoparticle-functionalized BNNTs have not been frequent in the literature. Only recently have several pioneering works been reported in this field. Han et al. filled one-dimensional potassium halide crystals in BNNTs by annealing the crystal-tube mixtures.<sup>9</sup> In experiments by Golberg et al., as-grown BNNTs were found to encapsulate MgO or metals.<sup>10–11</sup> A stannic oxide was coated on BNNTs by a wet chemistry method,<sup>12</sup> which is practically important since SnO<sub>2</sub> can be used as a conductive electrode and as a transparent coating and has applications in heterojunction solar cells and in chemical sensors.<sup>13–14</sup> However, BNNTs which were previously used for SnO<sub>2</sub> coating were fabricated through a CNTs substitution reaction, thus they might be carbon contaminated. Also, only transmission electron spectroscopy

(TEM) characterization results were presented, while a detailed analysis of the composite physical properties was absent.

In this paper, pure BNNTs were synthesized at a high yield by a carbon-free chemical vapor deposition method with boron and metal oxide as the precursors (BOCVD).<sup>15–16</sup> SnO<sub>2</sub> was coated on a BNNT surface and filled into the tube channels using a wet chemistry method. Detailed characterization of the functionalized BNNTs reveals the prominent variations in the particle and tube atomic and electronic structures after functionalization.

## Experimental Section

Gram quantities of BNNTs were synthesized by the carbon-free BOCVD method.<sup>15–16</sup> A mixture of MgO, FeO, and boron powder was used as the precursor, and NH<sub>3</sub> was used as the nitrogen source. The as-grown samples were washed by HNO<sub>3</sub> to remove catalyst and impurities. The purified samples typically contained nanotubes with diameters of ~20–50 nm and lengths of up to 10 μm. After purification, the tube fraction in the samples may reach more than 90 vol %. The general method adopted to functionalize BNNTs with SnO<sub>2</sub> was similar to that of the Han's experiments.<sup>12</sup> However, in our experiments, the mixtures of HCl, BNNTs, and SnCl<sub>2</sub> were stirred and heated to 100 °C instead of sonication. After 5 h reaction, the samples were washed with distilled water several times and dried before further characterization.

TEM analysis was performed using a JEOL-3000F and JEOL-3100FEF high-resolution field-emission TEM operated at 300 kV. The samples were made by dispersing BNNT–SnO<sub>2</sub> in ethanol and dripping the mixtures onto carbon-coated copper grids, followed by ethanol evaporation. The phase structure of the product was characterized by X-ray diffraction (XRD) using a RINT2200 diffractometer with standard Cu Kα radiation. The UV–vis absorption experiments were performed using a HITACHI U-4100 spectrometer.

\* To whom correspondence should be addressed. Tel: 81-29-851-3354 (8659 ext.). Fax: 81-29-851-6280. E-mail: zhi.chunyi@nims.go.jp.

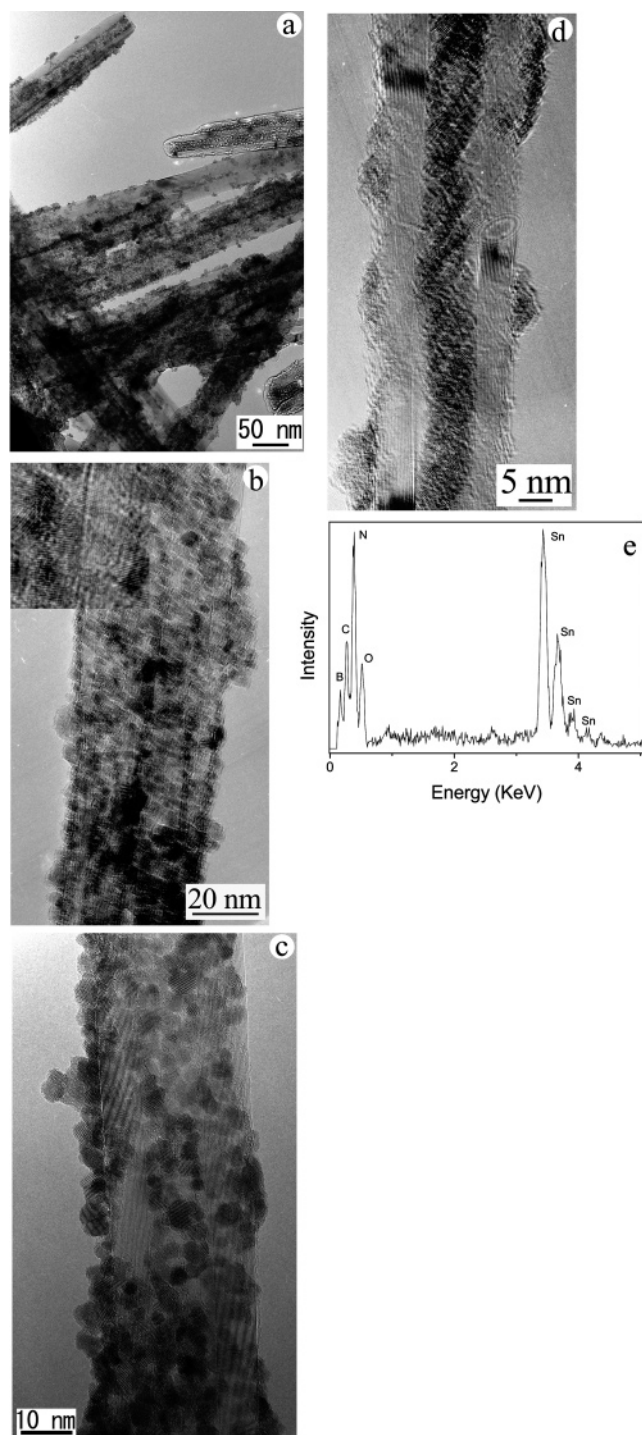


**Figure 1.** (a) Low magnification TEM image of BNNT covered with SnO<sub>2</sub> nanoparticles; (b) TEM image of a BNNT fully covered with SnO<sub>2</sub> nanoparticles; the inset is the enlarged image showing that the particle is well-crystalline; (c) TEM image of a partially covered BNNT; (d) TEM image of a BNNT filled with a SnO<sub>2</sub> phase; (e) EDS of the BNNT-SnO<sub>2</sub> nanocomposite shown in (c), the carbon-related signal is from a carbon-coated Cu grid.

## Results and Discussion

All BNNTs were covered by SnO<sub>2</sub>, nearly 50% were fully coated, while the other fraction was partially covered, as shown in parts a, b, and c of Figure 1. The difference in these two kinds of BNNTs is still unclear since the interaction mechanism between BNNTs and SnO<sub>2</sub> requires further studies. The SnO<sub>2</sub> on the surface of BNNTs is highly crystalline nanoparticle, with the diameters 1.5 to 7 nm, as shown in the inset to Figure 1b. It

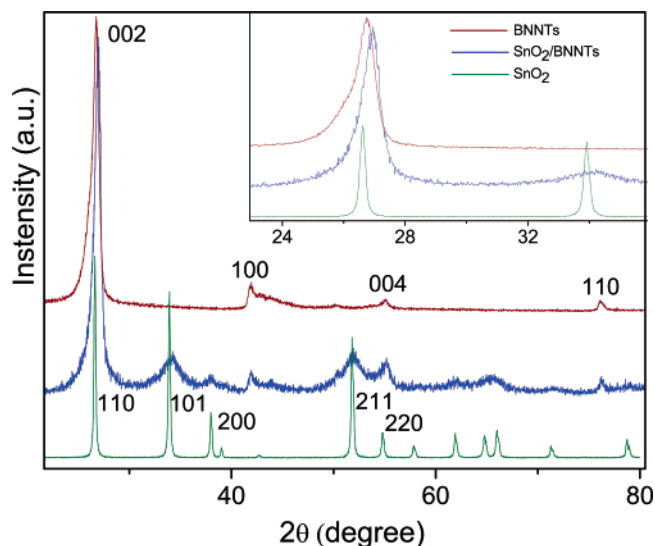


**Figure 2.** Comparative XRD of BNNTs, a BNNT-SnO<sub>2</sub> nanocomposite, and a commercially available SnO<sub>2</sub> powder. It is clear that the material on BNNTs is SnO<sub>2</sub>. The inset is the enlarged portion showing the shifts of the XRD peaks.

was found that some SnO<sub>2</sub> particles were filled in BNNTs due to numerous open tip-ends in the purified BNNTs, particularly well seen in the partially covered BNNTs, as shown in Figure 1d. This means that wet chemistry may be an effective method to fill BNNTs, although BNNTs are hardly wetted by most of chemicals and materials according to the previous reports. Keeping in mind the chemical inertness and structural stability of BNNTs, these tubes may ensure the perfect protection of the materials embedded. The internal channels of BNNTs may also serve as nanoscale chambers/reactors to perform delicate chemical experiments in a confined space. The chemical composition of the functionalized BNNTs was investigated by energy-dispersive X-ray spectroscopy (EDS), as shown in Figure 1e. The result confirms the presence of B, N, O, and Sn. The atomic ratio of O to Sn is close to 2.

Figure 2 shows the XRD pattern of the as-prepared sample. Although some SnO<sub>2</sub>-related peaks overlap with those peculiar to BNNTs', the SnO<sub>2</sub> phase can be clearly identified using several isolated peaks. The SnO<sub>2</sub>-related peaks are broad, which indicates that the particle size is very small. This is consistent with the TEM observations. A SnO impurity phase, which appeared in Han's experiment,<sup>12</sup> was absent in the present material. In addition, no peaks corresponding to Sn and SnCl<sub>2</sub> impurity phases were observed. This difference in the sample quality may be due to the different experimental procedures adopted.

A novel phenomenon observed in our experiments is the notable shift of XRD peaks. As shown in Figure 2, the SnO<sub>2</sub>(101) and (211) peaks shift to the higher diffraction angles compared with the peak positions for a commercially available SnO<sub>2</sub> powder. This indicates that an interplanar distance of SnO<sub>2</sub> nanoparticles functionalized on BNNTs becomes smaller. Also, the peaks corresponding to the BNNT(002) plane and the SnO<sub>2</sub>(110) plane markedly shift to the higher diffraction angles. Since the intensity of SnO<sub>2</sub>-related peaks is much weaker compared with that of BNNTs, this shift is thought to originate from the corresponding lattice distance variations within both BNNT(002) and SnO<sub>2</sub>(110) planes. This phenomenon was not observed in the previous studies on SnO<sub>2</sub> nanomaterials, therefore, it is suggested that the shift originates from the strong interactions between BNNTs and SnO<sub>2</sub> nanoparticles. These interactions may result in a compressive stress, which changes

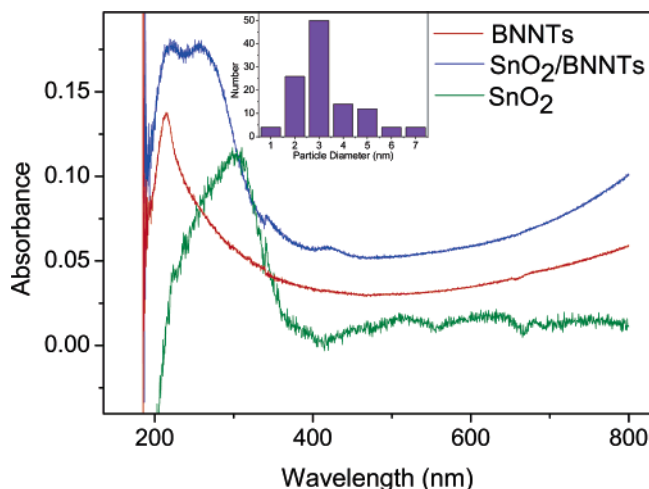


**Figure 3.** Comparative UV-vis absorption spectra of BNNTs, a BNNT-SnO<sub>2</sub> nanocomposite, and a commercially available SnO<sub>2</sub> powder. The shift of the SnO<sub>2</sub>-related peak is obvious. The inset is statistical data to the SnO<sub>2</sub> nanoparticles diameter distribution.

an interplanar distance.<sup>17</sup> For BNNTs, only the (002) plane may be in a physical contact with the SnO<sub>2</sub> particles. Thus, the stresses must be along the direction perpendicular to the (002) plane resulting in a (002) peak shift. However, for SnO<sub>2</sub> nanoparticles, any crystal planes may contact BNNTs, thus the clear shifts of the (110), (101), and (211) peaks were observed.

One type of possible interaction is the electrostatic interactions. Both BNNTs and SnO<sub>2</sub> are wide band gap semiconductors. During functionalization, the static charges may be accumulated on them. This induces the strong electrostatic interactions between the two phases. The other possibility is the formation of Sn-N bonds.<sup>18</sup> Our previous studies indicate that amide groups may exist on the surface of BNNTs,<sup>19</sup> thus an atomic layer containing the Sn-N bonds may form between the BNNTs and SnO<sub>2</sub> nanoparticles. The lattice mismatch may induce a compressive stress, which is responsible for the shift of XRD peaks. The investigations of a detailed interaction mechanism using high-sensitivity Fourier transform infrared spectroscopy are underway.

To properly reveal the variations in the electronic structure of the functionalized tubes, UV-vis absorption experiments were performed, as shown in Figure 3. The bulk SnO<sub>2</sub> has a band gap energy of 3.6 eV.<sup>20</sup> The corresponding UV-vis absorption spectrum shows a peak around 4.05 eV, whereas, for the SnO<sub>2</sub> nanoparticles functionalized on BNNTs, this peak shifts to 4.80 eV. This indicates that the band gap of SnO<sub>2</sub> had become wider. It is well-known that, when the dimensions of nanocrystalline particles approach the exciton Bohr radius, the quantum confinement effects will induce a blue shift in energy. The calculated electron Bohr radius of SnO<sub>2</sub> is around 2.7 nm,<sup>20</sup> which is comparable with the particle size observed in our experiments. It is suggested that the size effect is one of the possible reasons for the blue shift of the related UV-vis absorption peak. However, Lee et al.<sup>20</sup> while investigating the UV-vis absorption spectra of SnO<sub>2</sub> nanoparticles found that a band gap transition peak of SnO<sub>2</sub> had shifted to around 4.59 eV even when the mean particle diameter decreased to 1.75 nm. Interestingly, the blue shift observed in our experiments is

much larger (shift to 4.80 eV), while the particle size is bigger than 1.75 nm, as shown in the inset of Figure 3. It has been revealed that the strong interactions between BNNTs and SnO<sub>2</sub> particles change the structure of SnO<sub>2</sub>. The structure variations, in turn, may alter an electronic structure. Therefore, it is suggested that both the size effect and interaction between BNNTs and SnO<sub>2</sub> particles induce the blue shift of the UV-vis absorption peak. The change of BNNTs' UV-vis absorption peak cannot be straightforwardly identified because of peak broadening and overlapping.

## Conclusion

In summary, BNNTs were functionalized with SnO<sub>2</sub> nanoparticles via a simple wet chemistry method. The detailed TEM observations reveal that SnO<sub>2</sub> nanoparticles may cover the tube surface and be encapsulated in tube channels. The characteristic lattice distances of both BNNT and SnO<sub>2</sub> have been changed due to the strong interactions between them, which may imply the formation of Sn-N bonds or electrostatic tube/particle interactions. UV-vis absorption indicates that the band gap energy of SnO<sub>2</sub> particles is enlarged due to the size effects and interactions with BNNTs. The SnO<sub>2</sub>-coated and filled BNNTs nanocomposites may have enhanced gas sensitivity and are worth using as effective gas sensors. The optical properties made also be of significant interest due to the prominent variations in the electronic structure of the constituting phases.

**Acknowledgment.** The authors thank Drs. Y. Uemura, M. Mitome, K. Kurashima, R. Z. Ma, and T. Sasaki for their cooperation and kind help.

## References and Notes

- (1) Han, W. Q.; Zettl, A. *Nano Lett.* **2003**, *3*, 681.
- (2) Zhang, Y.; Franklin, N.; Chen, R.; Dai, H. *Chem. Phys. Lett.* **2000**, *35*, 331.
- (3) Fu, Q.; Lu, C.; Jie, L. *Nano Lett.* **2002**, *2*, 329.
- (4) Haremsa, J.; Hahn, M.; Krauss, T.; Chen, S.; Calcines, J. *Nano Lett.* **2002**, *2*, 1253.
- (5) Blase, X.; Rubio, A.; Louie, S. G.; Cohen, M. L. *Europhys. Lett.* **1994**, *28*, 335.
- (6) Golberg, D.; Bando, Y.; Kurashima, K.; Sato, T. *Scr. Mater.* **2001**, *44*, 1561.
- (7) Hernández, E.; Goze, C.; Bernier, P.; Rubio, A. *Phys. Rev. Lett.* **1998**, *80*, 4502.
- (8) Kim, P.; Shi, L.; Majumdar, A.; McEuen, P. L. *Phys. Rev. Lett.* **2001**, *87*, 215502.
- (9) Han, W. Q.; Chang, C. W.; Zettl, A. *Nano Lett.* **2004**, *4*, 1355.
- (10) Golberg, D.; Xu, F. F.; Bando, Y. *Appl. Phys. A* **2003**, *76*, 479.
- (11) Golberg, D.; Bando, Y.; Fushimi, K.; Mitome, M.; Bourgeois, L.; Tang, C. *J. Phys. Chem. B* **2003**, *107*, 8726.
- (12) Han, W. Q.; Zettl, A. *J. Am. Chem. Soc.* **2003**, *125*, 2062.
- (13) Kohl, D. *J. Phys. D* **2001**, *34*, R125.
- (14) Comini, E.; Faglia, G.; Sberveglieri, G.; Pan, Z.; Wang, Z. *Appl. Phys. Lett.* **2002**, *81*, 1869.
- (15) Tang, C.; Bando, Y.; Sato, T.; Kurashima, K. *Chem. Commun.* **2002**, 1290.
- (16) Zhi, C. Y.; Bando, Y.; Tang, C.; Golberg, D. *Solid State Commun.* **2005**, *135*, 67.
- (17) Hee, S. W.; Seung, B. Y.; Jeunghye, P.; Hyunik, Y.; Kwang, P. S.; Sangsig, K. *J. Chem. Phys.* **2002**, *116*, 9492.
- (18) Zhang, F.; Wang, X.; Li, C.; Li, X.; Wan, Q.; Xian, Y.; Jin, L.; Yamamoto, K. *Anal. Bioanal. Chem.* **2005**, *382*, 1368.
- (19) Zhi, C. Y.; Bando, Y.; Tang, C.; Honda, S.; Sato, K.; Kuwahara, H.; Golberg, D. *Angew. Chem., Int. Ed.* **2005**, *44*, 7932.
- (20) Lee, E. J. H.; Ribeiro, C.; Giralaldi, T. R.; Longo, E.; Leite, E. R.; Varela, J. A. *Appl. Phys. Lett.* **2004**, *84*, 1745.